Inorg. Chem. **2006**, *45*, 1543–1551

Novel Oxygen Chirality Induced by Asymmetric Coordination of an Ether Oxygen Atom to a Metal Center in a Series of Sugar-Pendant Dipicolylamine Copper(II) Complexes

Yuji Mikata,*,† Yuko Sugai,‡ Makoto Obata,‡ Masafumi Harada,§ and Shigenobu Yano*,‡

KYOUSEI Science Center, Division of Material Science, and Faculty of Human Life and Environment, Nara Women's University, Nara 630-8506, Japan

Received September 5, 2005

Six sugar-pendant 2,2′-dipicolylamine (DPA) ligands (**L1**–**3** and **L′1**–**3**) have been prepared. OH-protected and unprotected D-glucose, D-mannose, and D-xylose were attached to a DPA moiety via an *O*-glycoside linkage. X-ray crystallography of the copper(II) complexes (**1**–**5**) with these ligands revealed that the anomeric oxygen atom is coordinated to the metal center in the solid state, generating a chiral center at the oxygen atom. The CD spectra of these copper complexes in methanol or aqueous solution exhibit Cotton effects in the d–d transition region, which indicates that the ether oxygen atoms remain coordinated to the metal center and the oxygen-atom chirality is preserved even in solution. For complexes **1** and **2**, the inverted oxygen-atom chirality and chelate-ring conformation in the solid state are well correlated with the mirror-image CD spectra in methanol solution. The concomitant inversion of the asymmetric configuration around the copper center was also observed in a methanol solution of complex **3** and a pyridine solution of complex **2**. The square-pyramidal/octahedral copper(II) centers also exhibited characteristic absorption and CD spectra.

Introduction

It is well-known that a nitrogen lone pair inverts via pyramidal inversion,[1,2] causing expeditious loss of chirality at a stereogenic nitrogen center. Thus, asymmetric nitrogen atoms that have been characterized have been limited to a series of quaternary ammonium ions[3,4] and *N*-oxides,[5,6] protonated[7,8] or metal-coordinated[9−16] amine ligands, and free tertiary amines with adequate electronic[17] and structural[18,19] restrictions. Among them, asymmetric nitrogen atoms coordinated to metal centers are of particular interest as the chirality exists in the primary coordination sphere of the metal ion, potentially influencing the physical and chemical properties of the metal center.[16] At the same time, there is a close relationship between the nitrogen chirality and the whole asymmetric structure of the metal complex.[20−22]

* To whom correspondence should be addressed. Tel./fax: +81-742-20-3095 (Y.M.), +81-742-20-3392 (S.Y.). E-mail: mikata@cc.nara-wu.ac.jp (Y.M.), yano@cc.nara-wu.ac.jp (S.Y.).

† *KYOUSEI* Science Center.

‡ Division of Material Science.

§ Faculty of Human Life and Environment.

(1) Belostotskii, A. M.; Gottlieb, H. E.; Aped, P. *Chem. Eur. J.* **2002**, *8*, 3016.
(2) Belostotskii, A. M.; Gottlieb, H. E.; Shokhen, M. *J. Org. Chem.* **2002**, *67*, 9257.
(3) Ooi, T.; Maruoka, K. *Acc. Chem. Res.* **2004**, *37*, 526.
(4) Lygo, B.; Andrews, B. I. *Acc. Chem. Res.* **2004**, *37*, 518.
(5) Goldberg, S. I.; Lam, F.-L. *J. Am. Chem. Soc.* **1969**, *91*, 5113.
(6) Muntz, R. L.; Pirkle, W. H.; Paul, I. C. *J. Chem. Soc., Perkin Trans. 2* **1972**, 483.
(7) Bonnot, C.; Chambron, J.-C.; Espinosa, E. *J. Am. Chem. Soc.* **2004**, *126*, 11412.
(8) Wash, P. L.; Renslo, A. R.; Rebek, J., Jr. *Angew. Chem., Int. Ed.* **2001**, *40*, 1221.
(9) Buckingham, D. A.; Marzilli, L. G.; Sargeson, A. M. *J. Am. Chem. Soc.* **1967**, *89*, 825.
(10) Yamaguchi, M.; Yano, S.; Saburi, M.; Yoshikawa, S. *Inorg. Chem.* **1980**, *19*, 2016.
(11) Okamoto, K.; Okabayashi, M.; Ohmasa, M.; Einaga, H.; Hidaka, J. *Chem. Lett.* **1981**, 725.
(12) Sakagami, N.; Yasui, T.; Kawaguchi, H.; Ama, T.; Kaizaki, S. *Bull. Chem. Soc. Jpn.* **1994**, *67*, 680.
(13) Murmann, R. K.; Barnes, C. L.; Barakat, S. *Polyhedron* **2001**, *20*, 431.
(14) Erickson, L. E.; Fritz, H. L.; May, R. J.; Wright, D. A. *J. Am. Chem. Soc.* **1969**, *91*, 2513.
(15) Lee, C.-S.; Wang, G.-T.; Chung, C.-S. *J. Chem. Soc., Dalton Trans.* **1984**, 109.
(16) Pelz, K. A.; White, P. S.; Gagné, M. R. *Organometallics* **2004**, *23*, 3210.
(17) Kostyanovsky, R. G.; Rudchenko, V. F.; Shtamburg, V. G.; Chervin, I. I.; Nasibov, S. S. *Tetrahedron* **1981**, *37*, 4245.
(18) Shustov, G. V.; Kadorkina, G. K.; Kostyanovsky, R. G.; Rauk, A. *J. Am. Chem. Soc.* **1988**, *110*, 1719.
(19) Hoffmann, H. M. R.; Frackenpohl, J. *Eur. J. Org. Chem.* **2004**, 4293.
(20) Buckingham, D. A.; Mason, S. F.; Sargeson, A. M.; Turnbull, K. R. *Inorg. Chem.* **1966**, *5*, 1649.

10.1021/ic051513f CCC: $33.50
Published on Web 01/28/2006

Similarly, it is possible that the oxygen atom of an unsymmetrical ether can become a chiral center when coordinated to a metal ion. In this case also, the chirality is extremely unstable because of the rapid inversion of the remaining oxygen lone pair. Preventing lone-pair inversion by metal ion coordination is a potential route to compounds exhibiting chiral oxygen atoms. Strong coordination of the metal ion to the ether oxygen atom can lead to the necessary differentiation of the two oxygen lone pairs. Careful ligand design is needed in any effort to isolate a compound with a metal-bound asymmetric oxygen atom.

The interaction of metal ions with carbohydrates is an important element for biochemical processes. The investigation of metal complexes involving carbohydrates should clarify many functions of carbohydrates in natural systems.[23−25] Carbohydrate-conjugated metal complexes also exhibit several bioactivities. Medicinal applications of carbohydrate−transition metal complexes include cisplatin derivatives[26−29] and nuclear imaging/therapy.[30−33] Carbohydrates as a metalloligand are of significant interest not only in bioinorganic chemistry but also in basic coordination chemistry.[34−37] During our program to study sugar−metal interactions using *O*-glycoside pendant ligands, we have found that the anomeric oxygen atom is capable of coordination to the metal center,[38,39] resulting in a chiral center. The crystal structures of the copper(II)-bound anomeric oxygen atom of two sugar-pendant DPA (dipicolylamine) ligands **L1** and **L′1** (Chart 1) exhibit a chiral oxygen atom with opposite configurations. Interestingly, this chirality and the chelate-ring conformation were determined to remain in methanol solution by mirror-image CD spectra.[39] Steric repulsion and an attractive force were properly used in this system. To the best of our knowledge, oxygen-atom chirality has never before been discussed explicitly, although a number of crystal structures of metal-coordinated asymmetric ethers (R−O−R′),[40−46] including metal-bound oxygen-containing macrocycles (crown ethers or cryptands),[47−53] have been reported. In this article, controlling factors for the assembly of asymmetric oxygen atoms are discussed, including the effect of a sugar moiety, counterion, and solvent in a series of sugar-pendant dipicolylamine copper(II) complexes.

Chart 1

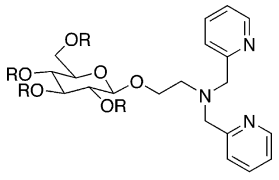

L1: R = Ac
L′1: R = H

Experimental Section

General Information. ^{1}H (300.07 Hz) and ^{13}C (75.45 Hz) NMR spectra were recorded on a Varian GEMINI 2000 spectrometer and referenced to internal TMS or solvent signals. UV−vis and CD spectra were measured on a Jasco V-570 spectrophotometer and Jasco J-720 spectropolarimeter using spectrograde solvent (Wako Pure Chemicals, Inc.). IR spectra were recorded on a Shimadzu FTIR-8700 spectrometer as KBr disks. Electrospray ionization mass spectrometry (ESI-MS) data were recorded on a JEOL JMS-T100LC instrument. Elemental analyses were carried out using a Perkin-Elmer PE2400 Series II CHNS/O analyzer (Nara Institute of Science and Technology). ***Caution****: Perchlorate salts of metal complexes with organic ligands are potentially explosive. All due precautions should be taken.*

***N,N*-Bis(2-pyridylmethyl)-2-aminoethyl 2,3,4,6-tetra-*O*-acetyl-*β*-D-glucopyranoside (L1).** 2-Bromoethyl 2,3,4,6-tetra-*O*-acetyl-*β*-D-glucopyranoside (2.08 g, 4.56 mmol), 2,2′-dipicolylamine (DPA) (0.90 g, 4.54 mmol), and potassium carbonate (2.52 g, 18.3 mmol) were mixed in *N*,*N*-dimethylformamide (5 mL). The mixture was stirred for 4 days at room temperature. The reaction mixture was extracted with $CHCl_3$, and the organic phase was washed with

(21) Saburi, M.; Homma, M.; Yoshikawa, S. *Inorg. Chem.* **1969**, *8*, 367.
(22) Ajioka, M.; Yano, S.; Matsuda, K.; Yoshikawa, S. *J. Am. Chem. Soc.* **1981**, *103*, 2459.
(23) Lis, H.; Sharon, N. *Chem. Rev.* **1998**, *98*, 637.
(24) Sears, P.; Wong, C.-H. *Angew. Chem., Int. Ed.* **1999**, *38*, 2300.
(25) Wong, C.-H. *Acc. Chem. Res.* **1999**, *32*, 376.
(26) Tsubomura, T.; Ogawa, M.; Yano, S.; Kobayashi, K.; Sakurai, T.; Yoshikawa, S. *Inorg. Chem.* **1990**, *29*, 2622.
(27) Hanessian, S.; Wang, J. *Can. J. Chem.* **1993**, *71*, 886.
(28) Chen, Y.; Heeg, M. J.; Braunschweiger, P. G.; Xie, W.; Wang, P. G. *Angew. Chem., Int. Ed.* **1999**, *38*, 1768.
(29) Mikata, Y.; Shinohara, Y.; Yoneda, K.; Nakamura, Y.; Brudziñska, I.; Tanase, T.; Kitayama, T.; Takagi, R.; Okamoto, T.; Kinoshita, I.; Doe, M.; Orvig, C.; Yano, S. *Bioorg. Med. Chem. Lett.* **2001**, *11*, 3045.
(30) Petrig, J.; Schibli, R.; Dumas, C.; Alberto, R.; Schubiger, P. A. *Chem. Eur. J.* **2001**, *7*, 1868.
(31) Storr, T.; Fisher, C. L.; Mikata, Y.; Yano, S.; Adam, M. J.; Orvig, C. *Dalton Trans.* **2005**, 654.
(32) Storr, T.; Sugai, Y.; Barta, C. A.; Mikata, Y.; Adam, M. J.; Yano, S.; Orvig, C. *Inorg. Chem.* **2005**, *44*, 2698.
(33) Storr, T.; Obata, M.; Fisher, C. L.; Bayly, S. R.; Green, D. E.; Brudziñska, I.; Mikata, Y.; Patrick, B. O.; Adam, M. J.; Yano, S.; Orvig, C. *Chem. Eur. J.* **2005**, *11*, 195.
(34) Yano, S., Otsuka, K., Sigel, H., Sigel, S., Eds.; Marcel Dekker: New York, 1996; p 27.
(35) Whitfield, D. M.; Stojkovski, S.; Sarkar, B. *Coord. Chem. Rev.* **1993**, *122*, 171.
(36) Yano, S. *Coord. Chem. Rev.* **1988**, *92*, 113.
(37) Gyurcsik, B.; Nagy, L. *Coord. Chem. Rev.* **2000**, *203*, 81.
(38) Yano, S.; Shinohara, Y.; Mogami, K.; Yokoyama, M.; Tanase, T.; Sakakibara, T.; Nishida, F.; Mochida, K.; Kinoshita, I.; Doe, M.; Ichihara, K.; Naruta, Y.; Mehrkhodavandi, P.; Buglyó, P.; Song, B.; Orvig, C.; Mikata, Y. *Chem. Lett.* **1999**, 255.
(39) Mikata, Y.; Sugai, Y.; Yano, S. *Inorg. Chem.* **2004**, *43*, 4778.
(40) Al-Mandhary, M. R. A.; Steel, P. J. *Eur. J. Inorg. Chem.* **2004**, 329.
(41) Kawano, T.; Kuwana, J.; Du, C.-X.; Ueda, I. *Inorg. Chem.* **2002**, *41*, 4078.
(42) Osa, S.; Sunatsuki, Y.; Yamamoto, Y.; Nakamura, M.; Shimamoto, T.; Matsumoto, N.; Re, N. *Inorg.* Chem. **2003**, *42*, 5507.
(43) Su, C.-Y.; Liao, S.; Wanner, M.; Fiedler, J.; Zhang, C.; Kang, B.-S.; Kaim, W. *Dalton Trans.* **2003**, 189.
(44) Al-Mandhary, M. R. A.; Steel, P. J. *Inorg. Chim. Acta* **2003**, *351*, 7.
(45) Shova, S.; Novitchi, G.; Gdaniec, M.; Caneschi, A.; Gatteschi, D.; Korobchenko, L.; Voronkova, V. K.; Simonov, Y. A.; Turta, C. *Eur. J. Inorg. Chem.* **2002**, 3313.
(46) Bu, X.-H.; Liu, H.; Du, M.; Wong, K. M.-C.; Yam, V. W.-W. *Inorg. Chim. Acta* **2002**, *333*, 32.
(47) Ma, S.-L.; Zhu, W.-X.; Gao, S.; Guo, Q.-L.; Xu, M.-Q. *Eur. J. Inorg. Chem.* **2004**, 1311.
(48) Mukhopadhyay, P.; Sarkar, B.; Bharadwaj, P. K.; Nättinen, K.; Rissanen, K. *Inorg. Chem.* **2003**, *42*, 4955.
(49) Belohradsky, M.; Budesinsky, M.; Cisarova, I.; Dekoj, V.; Holy, P.; Zavada, J. *Tetrahedron* **2003**, *59*, 7751.
(50) Autzen, S.; Korth, H.-G.; Boese, R.; de Groot, H.; Sustmann, R. *Eur. J. Inorg. Chem.* **2003**, 1401.
(51) Mao, J.-G.; Wang, Z.; Clearfield, A. *Inorg. Chem.* **2002**, *41*, 3713.
(52) Fenton, R. R.; Gauci, R.; Junk, P. C.; Lindoy, L. F.; Luckay, R. C.; Meehan, G. V.; Price, J. R.; Turner, P.; Wei, G. *Dalton Trans.* **2002**, 2185.
(53) Tei, L.; Blake, A. J.; Bencini, A.; Valtancoli, B.; Wilson, C.; Schröder, M. *Inorg. Chim. Acta* **2002**, *337*, 59.

water, dried over Na_2SO_4, and concentrated. The crude product was purified by silica gel column chromatography (eluent, ethyl acetate/MeOH = 1:0−10:1 + 0.1% v/v acetic acid). Yield: 2.05 g (78%) as an oily product. ESI-MS(methanol): *m*/*z* $[M + H]^+$ 574.2. ^{1}H NMR (300.07 MHz, $CDCl_3$) δ (ppm): 8.51 (m, 2H, ^3J = 3.3 Hz, py-H6), 7.67 (dt, 2H, ^3J = 7.5 Hz, ^4J = 1.8 Hz, py-H4), 7.54 (d, 2H, ^3J = 7.8 Hz, py-H3), 7.17−7.13 (m, 2H, py-H5), 5.21 (t, 1H, ^3J = 9.3 Hz, H3), 5.08−4.99 (m, 2H, H2, H4), 4.56 (d, 1H, ^3J = 7.8 Hz, H1), 4.26 (dd, 1H, ^3J = 4.6 Hz, ^2J = 12.4 Hz, H6a), 4.10 (dd, 1H, ^3J = 2.4 Hz, ^2J = 12.0 Hz, H6b), 3.97−4.00 (m, 1H, OCH_2), 3.87 (s, 4H, CH_2Py), 3.66−3.73 (m, 2H, H5, OCH_2), 2.83−2.84 (m, 2H, CH_2CH_2N), 2.05 (s, 3H, CH_3CO), 2.04 (s, 3H, CH_3-CO), 2.02 (s, 3H, CH_3CO), 1.96 (s, 3H, CH_3CO). ^{13}C NMR (75.45 MHz, $CDCl_3$) δ (ppm): 170.74 (C═O), 170.38 (C═O), 169.51 (C═O), 169.41 (C═O), 159.62 (py-C2), 149.01 (py-C6), 136.52 (py-C4), 122.93 (py-C3), 121.99 (py-C5), 100.54 (C1), 72.83 (C3), 71.63 (C5), 71.17, 68.29 (C2,4), 67.79 (OCH_2), 61.81 (C6), 60.48 (CH_2Py), 53.11 (CH_2CH_2N), 20.52 (CH_3), 20.40 (CH_3).

***N,N*-Bis(2-pyridylmethyl)-2-aminoethyl 2,3,4,6-tetra-*O*-acetyl-α-D-mannopyranoside (L2).** A reaction of 2-bromoethyl 2,3,4,6-tetra-*O*-acetyl-α-D-mannopyranoside (2.06 g, 4.52 mmol) with DPA (0.91 g, 4.6 mmol) in the presence of potassium carbonate (2.52 g, 18.25 mmol) in dimethylformamide (5 mL) with a workup similar to that described above gave **L2** (685 mg, 26%) as an oily material. ESI-MS (methanol): *m*/*z* 596.2 $[M + Na]^+$. ^{1}H NMR (300.07 MHz, $CDCl_3$) δ (ppm): 8.53 (m, 2H, py-H6), 7.72 (m, 2H, py-H4), 7.60 (d, 2H, py-H3), 7.18−7.14 (m, 2H, py-H5), 5.39−5.35 (m, 1H, H3), 5.31−5.24 (m, 2H, H2,4), 4.77 (d, 1H, J = 1.5 Hz, H1), 4.21 (m, 1H, H6a), 4.12 (dd, 1H, H6b), 4.03−3.96 (m, 1H, H5), 3.90 (d, 4H, CH_2Py), 3.85−3.83 (m, 1H, OCH_2), 3.58−3.56 (m, 1H, OCH_2), 2.88−2.85 (m, 2H, CH_2CH_2N), 2.16 (s, 3H, CH_3CO), 2.05 (s, 6H, CH_3CO), 2.02 (s, 3H, CH_3CO). ^{13}C NMR (75.45 MHz, $CDCl_3$) δ (ppm): 170.77 (C═O), 170.20 (C═O), 170.06 (C═O), 169.80 (C═O), 159.33 (py-C2), 149.11 (py-C6), 136.88 (py-C4), 122.91 (py-C3), 122.20 (py-C5), 97.63 (C1), 69.46 (C2 or 4), 69.11 (C3), 68.39 (C5), 66.03 (C2 or 4), 65.58 (C6), 62.34 (OCH_2), 60.56 (CH_2Py), 53.23 (CH_2CH_2N), 20.76 (CH_3), 20.57 (CH_3).

***N,N*-Bis(2-pyridylmethyl)-2-aminoethyl 2,3,4-tri-*O*-acetyl-β-D-xylopyranoside (L3).** A reaction of 2-bromoethyl 2,3,4-tri-*O*-acetyl-β-D-xylopyranoside (591 mg, 1.54 mmol) with DPA (309 mg, 1.55 mmol) in the presence of potassium carbonate (859 mg, 6.21 mmol) in dimethylformamide (3 mL) with a workup similar to that described above gave **L3** (167 mg, 22%) as an oily material. ESI-MS (methanol): *m*/*z* 502.3 $[M + H]^+$, 524.3 $[M + Na]^+$. ^{1}H NMR (300.07 MHz, $CDCl_3$) δ (ppm): 8.53 (d, 2H, py-H6), 7.68 (m, 2H, py-H4), 7.56 (d, 2H, py-H3), 7.19−7.14 (m, 2H, py-H5), 5.15 (t, 1H, H3), 4.97−4.90 (m, 2H, H2, H4), 4.49 (d, 1H, J = 7.2 Hz, H1), 4.09 (dd, 1H, H5a), 3.91−3.96 (m, 1H, OCH_2), 3.88 (s, 4H, CH_2Py), 3.63−3.66 (m, 1H, OCH_2), 3.34 (dd, 1H, H5b), 2.82 (t, 2H, CH_2CH_2N), 2.05 (s, 3H, CH_3CO), 2.02 (s, 3H, CH_3CO), 1.99 (s, 3H, CH_3CO). ^{13}C NMR (75.45 MHz, $CDCl_3$) δ (ppm): 170.05 (C═O), 169.81 (C═O), 169.39 (C═O), 159.36 (py-C2), 148.59 (py-C6), 136.77 (py-C4), 122.99 (py-C3), 122.03 (py-C5), 100.48 (C1), 71.55 (C3), 70.74, 68.67 (C2, C4), 67.54 (OCH_2), 61.81 (C5), 60.32 (CH_2Py), 53.31 (CH_2CH_2N), 20.69 (CH_3), 20.54 (CH_3).

***N,N*-Bis(2-pyridylmethyl)-2-aminoethyl β-D-glucopyranoside (L′1).** To a methanol solution (11 mL) of **L1** (175 mg, 0.31 mmol) was added sodium methoxide, and the pH was adjusted to 9. The reaction mixture was stirred for 90 min at room temperature. Dowex 50 × $8H^+$ was added, and the pH was adjusted to 7. The reaction solution was filtered to remove resin, and solvent was removed in vacuo. Yield: 136 mg (∼100%). ESI-MS (methanol): *m*/*z* 406.2 $[M + H]^+$. ^{1}H NMR (300.07 MHz, D_2O) δ (ppm): 8.42 (m, 2H, py-H6), 7.78 (td, 2H, ^3J = 7.5 Hz, ^4J = 1.8 Hz, py-H4), 7.45 (d, 2H, ^3J = 7.8 Hz, py-H3), 7.29−7.33 (m, 2H, py-H5), 4.39 (d, 1H, ^3J = 7.8 Hz, H1), 4.02 (m, 1H, OCH_2), 3.86−3.91 (m, 1H, H6a), 3.83 (s, 4H, CH_2Py), 3.67−3.80 (m, 3H, H5, H6b, OCH_2), 3.44−3.51 (m, 1H, ^3J = 7.5 Hz, H3), 3.39−3.40 (m, 1H, H4), 3.23−3.29 (m, 1H, H2), 2.85−2.88 (m, 2H, CH_2CH_2N). ^{13}C NMR (75.45 MHz, D_2O) δ (ppm): 159.86 (py-C2), 150.74 (py-C6), 140.59 (py-C4), 127.34 (py-C3), 125.70 (py-C5), 105.02 (C1), 78.49 (C3,C5), 75.85 (C2), 72.26 (C4), 69.87 (OCH_2), 63.41 (C6), 62.49 (CH_2-Py), 56.03 (CH_2CH_2N).

***N,N*-Bis(2-pyridylmethyl)-2-aminoethyl α-D-mannopyranoside (L′2).** A methanol solution (22 mL) of **L2** (299 mg, 0.5 mmol) was treated as described above to give **L′2** (225 mg, ∼100%). ESI-MS: *m*/*z* 428.1 $[M + Na]^+$. ^{1}H NMR (300.07 MHz, D_2O) δ (ppm): 8.40−8.42 (m, 2H, py-H6), 7.75−7.82 (m, 2H, py-H4), 7.44−7.48 (m, 2H, py-H3), 7.30−7.34 (m, 2H, py-H5), 4.69 (s, 1H, H1), 3.50−3.84 (m, 8H, H2,H3,H4,H5,H6ab, OCH_2), 3.37 (s, 4H, CH_2Py), 2.84 (d, 2H, J = 5.4 Hz, CH_2CH_2N). ^{13}C NMR (75.45 MHz, D_2O) δ (ppm): 160.18 (py-C2), 150.72 (py-C6), 140.68 (py-C4), 127.09 (py-C3), 125.80 (py-C5), 102.45 (C1), 75.45, 73.28, 72.71, 69.36 (C2, C3, C4, C5), 67.56 (OCH_2), 63.52 (C6), 62.68 (CH_2Py), 56.10 (CH_2CH_2N).

***N,N*-Bis(2-pyridylmethyl)-2-aminoethyl β-D-xylopyranoside (L′3).** A methanol solution (22 mL) of **L3** (337 mg, 0.67 mmol) was treated as described above to give **L′3** (257 mg, ∼100%). ESI-MS: *m*/*z* 398.1 $[M + Na]^+$. ^{1}H NMR (300.07 MHz, D_2O) δ (ppm): 8.39 (d, 2H, J = 4.5 Hz, py-H6), 7.77 (t, 2H, py-H4), 7.42 (d, 2H, J = 7.8 Hz, py-H3), 7.29−7.32 (m, 2H, py-H5), 4.33 (d, 1H, J = 7.5 Hz, H1), 3.89−3.94 (m, 2H, H5a, OCH_2), 3.80 (s, 4H, CH_2Py), 3.73−3.77 (m, 1H, OCH_2), 3.56−3.61 (m, 1H, H4), 3.41 (dd, 1H, H3), 3.22−3.29 (m, 2H, H2, H5b), 2.84 (t, 2H, CH_2CH_2N). ^{13}C NMR (75.45 MHz, D_2O) δ (ppm): 157.41 (py-C2), 148.29 (py-C6), 138.15 (py-C4), 124.88 (py-C3), 123.31 (py-C5), 103.38 (C1), 75.90 (C3), 73.25 (C2), 69.48 (C4), 67.54 (OCH_2), 65.36 (C5), 60.06 (CH_2Py), 53.61 (CH_2CH_2N).

[Cu(L1)(NO_3)](NO_3) (1). To a methanol solution (3 mL) of **L1** (476 mg, 0.83 mmol) was added $Cu(NO_3)_2 \cdot 3H_2O$ (201 mg, 0.83 mmol) in methanol (3 mL) at room temperature. The solution was allowed to stand at 5 °C to precipitate **1**. Yield: 333 mg (53%). Anal. Calcd for $C_{28}H_{35}CuN_5O_{16}$ (**1**): C, 44.18; H, 4.63; O, 9.20. Found: C, 43.81; H, 4.63; N, 9.13. FABMS (NBA): *m*/*z* 698 [Cu**L1**NO_3]$^+$,636 [Cu**L1**]$^+$. HRMS (ESI): *m*/*z* = 636.1602 {calcd for $C_{28}H_{35}CuN_3O_{10}$ ([Cu**L1**]$^+$: 636.1613}.

[Cu(L′1)(CH_3COO)](NO_3)·$2H_2O$ (2·$2H_2O$). To a methanol solution (2 mL) of **L′1** (137 mg, 0.34 mmol) was added $Cu(NO_3)_2 \cdot 3H_2O$ (81 mg, 0.34 mmol) in methanol (2 mL) at room temperature. After addition of acetic acid (0.1 mL), the solution was allowed to stand at 5 °C to precipitate complex **2**. Yield: 28 mg (15%). Anal. Calcd for $C_{22}H_{34}CuN_4O_{13}$ (**2**·$2H_2O$): C, 42.21; H, 5.47; O, 8.95. Found: C, 42.53; H, 5.27; N, 9.14. FABMS (NBA) *m*/*z* 468 [Cu**L′1**]$^+$. HRMS (ESI): *m*/*z* = 467.1097 {calcd for $C_{20}H_{26}CuN_3O_6$ ([Cu**L′1** − H]$^+$): 467.1112}.

[Cu(L1)(ClO_4)(H_2O)](ClO_4)·H_2O (3·H_2O). To a methanol solution (2 mL) of **L1** (280 mg, 0.68 mmol) was added $Cu(ClO_4)_2 \cdot 6H_2O$ (256 mg, 0.69 mmol) in methanol (2 mL) at room temperature. The resulting solution was kept in the refrigerator with ether diffusion to precipitate complex **3** as a blue crystal. Yield: 110 mg (19%). ESI-MS (methanol): *m*/*z* 735.2 [Cu**L1**ClO_4]$^+$. Anal. Calcd for $C_{28}H_{37}O_{19}Cl_2CuN_3 \cdot H_2O$: C, 38.56; H, 4.51; N, 4.82. Found: C, 38.92; H, 4.40; N, 4.82. IR (KBr disk) ν (cm^{-1}): 1755, 1224, 1120−1036, 625.

[Cu(L′1)(CH_3COO)](ClO_4)·H_2O (4·H_2O). To a methanol solution (2 mL) of **L′1** (188 mg, 0.46 mmol) was added $Cu(ClO_4)_2 \cdot$

Table 1. Crystallographic Data for [Cu(**L1**)(ClO_4)(H_2O)](ClO_4) (**3**), [Cu(**L′1**)(CH_3COO)](ClO_4)·H_2O (**4**·H_2O), and [Cu(**L3**)(NO_3)(H_2O)](NO_3) (**5**)

	[Cu(**L1**)(ClO_4)(H_2O)](ClO_4) (**3**)	[Cu(**L′1**)(CH_3COO)](ClO_4)·H_2O (**4**·H_2O)	[Cu(**L3**)(NO_3)(H_2O)](NO_3) (**5**)
formula	$C_{28}H_{37}Cl_2N_3O_{19}Cu$	$C_{22}H_{32}ClN_3O_{13}Cu$	$C_{25}H_{33}N_5O_{15}Cu$
fw	854.06	645.51	707.11
crystal system	orthorhombic	orthorhombic	monoclinic
space group	$P2_12_12_1$	$P2_12_12_1$	$P2_1$
a, Å	13.4752(5)	8.7313(4)	9.679(9)
b, Å	15.5244(5)	15.8302(8)	15.577(13)
c, Å	17.1862(7)	19.5981(9)	10.177(9)
β, deg	90	90	96.650(5)
V, Å^3	3595.3(2)	2708.8(2)	1524.1(23)
Z	4	4	2
D_{calc}, g cm^{-3}	1.578	1.578	1.541
μ, cm^{-1}	8.404	9.760	7.969
$2\theta_{max}$, deg	55.0	55.0	55.0
temp, K	173	123	173
no. reflns collected	28064	21630	12786
no. reflns used	4522	3507	7116
no. of params	515	362	424
final R1 [$I > 2\theta(I)$][a]	0.033	0.048	0.046
wR2 (all data)[a]	0.075	0.131	0.108
GOF	0.981	1.075	0.964

[a] $R1 = \sum||F_o| - |F_c||/\sum|F_o|$. $wR2 = [\sum w[(F_o^2 - F_c^2)^2]/\sum[w(F_o^2)^2]]^{1/2}$.

$6H_2O$ (173 mg, 0.47 mmol) in methanol (1.5 mL) at room temperature. After addition of acetic acid (0.1 mL), the resulting solution was kept in the refrigerator to precipitate complex **4** as a blue crystal. Yield: 170 mg (57%). ESI-MS (methanol): m/z 467.2 [Cu**L′1** − H]$^+$. Anal. Calcd for $C_{22}H_{30}CuClN_3O_{12}$·$H_2O$: C, 40.94; H, 5.00; N, 6.51. Found: C, 40.43; H, 5.03: N, 6.25. IR (KBr disk) ν (cm^{-1}): 3527−2794, 1626, 1610, 1121, 1109−1032, 625.

[Cu(L3)(NO_3)(H_2O)](NO_3) (5). To a methanol solution (3 mL) of **L3** (242 mg, 0.48 mmol) was added $Cu(NO_3)_2$·$3H_2O$ (118 mg, 0.49 mmol) in methanol (2 mL) at room temperature. The resulting solution was kept in the refrigerator with ether diffusion to precipitate complex **5**. Yield: 45 mg (13%). ESI-MS (methanol): m/z 624.2 [Cu**L3**NO_3]$^+$, 564.2 [Cu**L3**]$^+$. Anal. Calcd for $C_{25}H_{33}CuN_5O_{15}$: C, 42.55; H, 4.57; N, 9.93. Found: C, 42.54; H, 4.73; N, 10.08. IR (KBr disk) ν (cm^{-1}): 3706−2596, 1755, 1612, 1384, 1298, 1248, 1229, 1163, 995−1125, 772.

X-ray Crystallography. Single crystals of **1**−**5** were covered by paraffin oil and mounted on a glass fiber. All diffractions were collected at 173 or 123 K on a Rigaku Mercury CCD detector, with monochromated Mo Kα radiation, operating at 50 kV/40 mA. Data were processed on a PC using CrystalClear software (Rigaku). Structures were solved by direct methods (SIR-97, SIR-92, or SHELXS-97) and refined by full-matrix least-squares methods on F^2 (SHELXS-97). Hydrogen atoms were calculated and treated with a riding model. The crystal data for **1** and **2** were reported previously.[39] Other crystal data are summarized in Table 1.

EXAFS Analysis. Extended X-ray absorption fine structure (EXAFS) measurements were performed at beam line 10B of Photon Factory of the High Energy Acceleration Research Organization (KEK−PF), Tsukuba, Japan. A channel-cut Si(311) monochromator was used. The ring current was 300−350 mA, and the storage ring was operated with an electron energy of 2.5 GeV. The experiments at the Cu K edge were carried out at room temperature in transmission mode with boron nitride for powdered samples of complexes **1** and **3**, methanol solution of complex **1**, and equimolar mixtures of **L2**−$Cu(NO_3)_2$ and **L3**−$Cu(NO_3)_2$ in methanol (∼0.1 M). The $\mathbf{k}^3\chi(\mathbf{k})$ value for the case of single scattering is theoretically given by eq 1

$$\mathbf{k}^3\chi(\mathbf{k}) = \sum_i \left\{ \frac{\mathbf{k}^2 N_i}{r_i^2} F_i(\mathbf{k}) \exp(-2\sigma_i^2\mathbf{k}^2) \sin[2\mathbf{k}r_i + \Phi(\mathbf{k})] \right\} \quad (1)$$

where r_i, N_i, $F_i(k)$, $\Phi_i(\mathbf{k})$, and σ_i represent the interatomic distance, the coordination number, the backscattering amplitude, the phase shift, and the Debye−Waller factor of the ith coordination shell, respectively, and $\mathbf{k}$ is the photoelectron wave vector defined as $\mathbf{k} = [(2m/\hbar)(E - E_0)]^{1/2}$ with the threshold energy E_0. The backscattering-amplitude [$F_i(\mathbf{k})$] and phase-shift [$\Phi_i(\mathbf{k})$] functions for corresponding bonds, such as between Cu and N/O atoms, were derived from complexes **1** and **3** as $N_{N/O} = 4 + 1$ and $4 + 2$, respectively, using the bond distances derived from X-ray crystallography. Parameters r_i, N_i, and σ_i were varied in nonlinear least-squares refined curve fitting by the use of the $F_i(\mathbf{k})$ and $\Phi_i(\mathbf{k})$ functions obtained above and fixed values of E_0 (8986 eV). All of the first-shell coordination atoms in 3N + 1O plane were treated as nitrogen. All calculations were performed with the EXAFS analysis program REX 2000 (Rigaku Co.).

Results and Discussion

Ligand Synthesis. One of the most common methodologies for the investigation of carbohydrate−metal ion interactions involves the use of sugar-pendant ligands.[29−33,38,54−58] The *O*-glycoside bond has been used extensively to synthesize sugar-pendant ligands, as this linkage is abundant in natural carbohydrates and easily constructed.[59,60] The sugar-pendant dipicolylamine (DPA) ligands **L1**−**3** were prepared from peracetylated pyranoses in two steps (Scheme 1). The first step involved the BF_3-catalyzed glycosylation of pen-

(54) Dumas, C.; Schibli, R.; Schubiger, P. A. *J. Org. Chem.* **2003**, *68*, 512.
(55) Mikata, Y.; Shinohara, Y.; Yoneda, K.; Nakamura, Y.; Esaki, K.; Tanahashi, M.; Brudziñska, I.; Hirohara, S.; Yokoyama, M.; Mogami, K.; Tanase, T.; Kitayama, T.; Takashiba, K.; Nabeshima, K.; Takagi, R.; Takatani, M.; Okamoto, T.; Kinoshita, I.; Doe, M.; Hamazawa, A.; Morita, M.; Nishida, F.; Sakakibara, T.; Orvig, C.; Yano, S. *J. Org. Chem.* **2001**, *66*, 3783.
(56) Song, B.; Mehrkhodavandi, P.; Buglyó, P.; Mikata, Y.; Shinohara, Y.; Yoneda, K.; Yano, S.; Orvig, C. *J. Chem. Soc., Dalton Trans.* **2000**, 1325.
(57) Mikata, Y.; Yoneda, K.; Tanase, T.; Kinoshita, I.; Doe, M.; Nishida, F.; Mochida, K.; Yano, S. *Carbohydr. Res.* **1998**, *313*, 175.
(58) Brudziñska, I.; Mikata, Y.; Obata, M.; Ohtsuki, C.; Yano, S. *Bioorg. Med. Chem. Lett.* **2004**, *14*, 2533.
(59) Bochkov, A. F., Zaikov, G. E., Eds. *Chemistry of the O-Glycosidic Bond: Formation & Cleavage*; Pergamon Press: Oxford, U.K., 1979.
(60) Capon, B. *Chem. Rev.* **1969**, *69*, 407.

Scheme 1

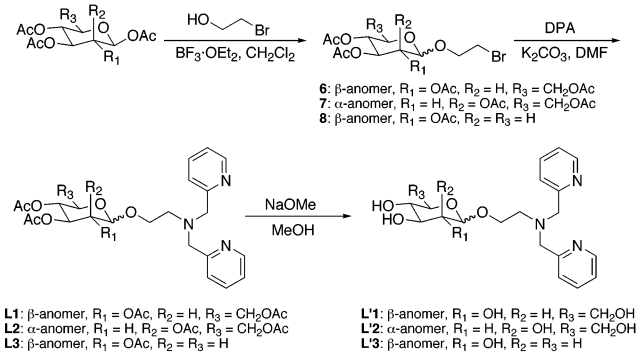

taacetyl-β-D-glucose, pentaacetyl-β-D-mannose, and tetraacetyl-β-D-xylose with 2-bromoethanol in dichloromethane. The protected bromoethyl glycosides **6**−**8** were then reacted with DPA in DMF in the presence of potassium carbonate at room temperature for 3−4 days. Purification by silica gel column chromatography (ethyl acetate + 0.1% v/v acetic acid) afforded pure **L1**−**3** as oily materials in 22−78% yield. Removal of the acetyl protecting groups by sodium methoxide afforded **L′1**−**3** quantitatively. All compounds were characterized by $^{1}H/^{13}C$ NMR spectroscopy and MS. The ligands **L′1**−**3** have recently been utilized to synthesize $^{99m}Tc/Re$ complexes as potential radiopharmaceuticals.[32] Several DPA-based ligands with a chiral moiety have been reported previously.[61−65]

Synthesis of Cu Complexes. Copper(II) complexes with **L1**−**3** and **L′1**−**3** were prepared in methanol solution using $Cu(NO_3)_2$ or $Cu(ClO_4)_2$ as a metal source. Upon mixing of the methanolic solutions of the ligand and copper salt, a color change from blue-green to dark blue was observed. Blue precipitates appeared in a few days in several cases, but many complexes remained in solution. Suitable crystals for X-ray crystallography were obtained only for $Cu(NO_3)_2$−**L1** (**1**), $Cu(ClO_4)_2$−**L1** (**3**), and $Cu(NO_3)_2$−**L3** (**5**) directly from methanol solution, and addition of few drops of acetic acid was effective for crystallization of $Cu(NO_3)_2$−**L′1** (**2**) and $Cu(ClO_4)_2$−**L′1** (**4**). Despite an extensive crystallization trial, no single crystals were obtained for the other copper complexes, although the complex formation in methanol solution was confirmed by ESI-MS.

Crystal Structures of Complexes 1−5. Figures 1−3 show the solid-state structures of the cations of complexes **3**−**5**. Crystal structures of complexes **1** and **2** were reported previously.[39] Complex **4** exhibited a structure almost identical to that of complex **2**, the only difference being the counterion (NO_3 vs ClO_4). Interestingly, all crystallized complexes exhibited coordination of the ether oxygen atom to the copper center. Coordination of one anion (nitrate for **1** and **5**, acetate for **2** and **4**, and perchlorate for **3**) to copper is also evident in the monocationic copper(II) complexes. Complexes **1**, **2**,

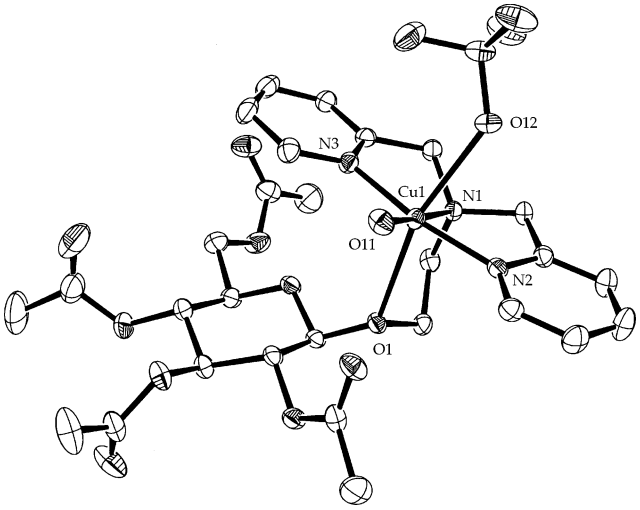

Figure 1. ORTEP plot for the cationic portion of [Cu(**L1**)(ClO_4)(H_2O)]-(ClO_4) (**3**). Selected bond lengths (Å): Cu1−N1 2.030(2), Cu1−N2 1.968-(3), Cu1−N3 1.959(3), Cu1−O1 2.537(2), Cu1−O11 1.978(2), Cu1−O12 2.525(2).

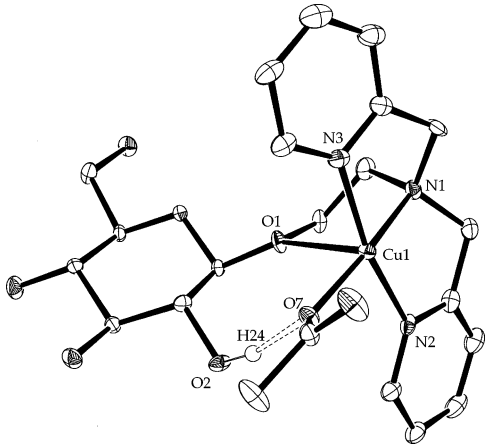

Figure 2. ORTEP plot for the cationic portion of [Cu(**L′1**)(CH_3COO)]-(ClO_4)·H_2O (**4**·H_2O). Selected bond lengths (Å): Cu1−N1 2.044(4), Cu1−N2 1.983(4), Cu1−N3 1.984(4), Cu1−O1 2.526(3), Cu1−O7 1.942(3).

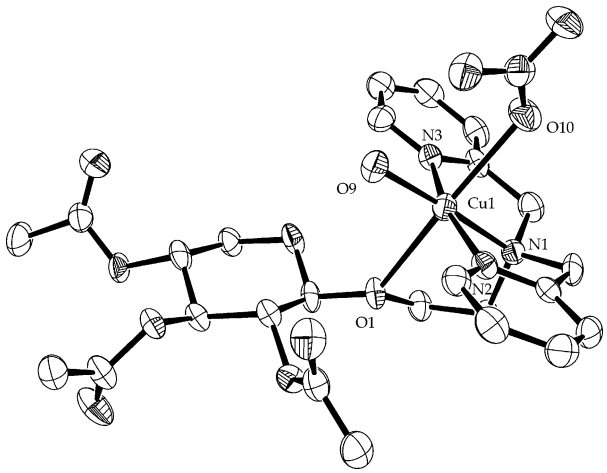

Figure 3. ORTEP plot for the cationic portion of [Cu(**L3**)(NO_3)(H_2O)]-(NO_3) (**5**). Selected bond lengths (Å): Cu1−N1 2.002(3), Cu1−N2 1.987-(3), Cu1−N3 1.975(3), Cu1−O1 2.534(2), Cu1−O9 1.960(3), Cu1−O10 2.454(3).

(61) Levadala, M. K.; Banerjee, S. R.; Maresca, K. P.; Babich, J. W.; Zubieta, J. *Synthesis*, **2004**, 1759.
(62) Yoshikawa, Y.; Kawabe, K.; Tadokoro, M.; Suzuki, Y.; Yanagihara, N.; Nakayama, A.; Sakurai, H.; Kojima, Y. *Bull. Chem. Soc. Jpn.* **2002**, *75*, 2423.
(63) Yamada, T.; Shinoda, S.; Uenishi, J.; Tsukube, H. *Tetrahedron Lett.* **2001**, *42*, 9031.
(64) Niklas, N.; Walter, O.; Alsfasser, R. *Eur. J. Inorg. Chem.* **2000**, 1723.
(65) Hartshorn, R. M.; Telfer, S. G. *J. Chem. Soc., Dalton Trans.* **2000**, 2801.

Table 2. Summary of the Coordination Environment of the Copper Center in Complexes **1**−**5** in the Crystal Structure

complex	coordination number	anomeric oxygen configuration	chelate-ring conformation
[Cu(**L1**)NO_3](NO_3) (**1**)	5	*R*	λ
[Cu(**L′1**)(CH_3COO)](NO_3) (**2**)	5	*S*	δ
[Cu(**L1**)(ClO_4)(H_2O)](ClO_4) (**3**)	6	*R*	δ
[Cu(**L′1**)(CH_3COO)](ClO_4) (**4**)	5	*S*	δ
[Cu(**L3**)(NO_3)(H_2O)](NO_3) (**5**)	6	*R*	λ

Table 3. Maximum Wavelength (nm) in the Absorption Spectra of Mixed Solutions of Copper Salts with **L1**−**3**, **L′1**−**3**, and Isolated Complexes **1**−**5** in Methanol or Aqueous Solution[a]

	in methanol		in water	
ligand or complex	$Cu(NO_3)_2$	$Cu(ClO_4)_2$	$Cu(NO_3)_2$	$Cu(ClO_4)_2$
L1	651 (**1**)	662 (**3**)	659 (**1**)	660 (**3**)
L2	649	664	653	653
L3	657 (**5**)	666	659 (**5**)	659
L′1	654 (**2**)	658 (**4**)	658 (**2**)	657 (**4**)
L′2	651	655	653	650
L′3	655	659	657	657
[Cu(**L1**)(NO_3)](NO_3) (**1**)	648		658	
[Cu(**L′1**)(CH_3COO)](NO_3) (**2**)	641		649	
[Cu(**L1**)(ClO_4)(H_2O)](ClO_4) (**3**)		661		658
[Cu(**L′1**)(CH_3COO)](ClO_4) (**4**)		639		647
[Cu(**L3**)(NO_3)(H_2O)](NO_3) (**5**)	649		657	

[a] Parentheses indicate the corresponding complex number.

and **4** crystallize in a five-coordinate square-pyramidal geometry, whereas complexes **3** and **5** exhibit six-coordinate distorted octahedral geometry, in which one water molecule occupies the sixth coordination site. For all complexes, the three nitrogen atoms of the DPA unit are coordinated to the copper center in a meridional fashion.[66−68] In the five-coordinate complexes (**1**, **2**, and **4**), the coordinated anion is located trans to the aliphatic nitrogen atom, leading to a distorted square-pyramidal coordination environment with the anomeric oxygen atom occupying the apical position. The hydrogen bond between O2 and counterion (O7) in **2** and **4** plays an important role in determining the complex structure.[39] In the six-coordinate complexes (**3** and **5**), the water molecule is located trans to the aliphatic nitrogen atom, and the oxygen atoms of the anomeric ether and counteranion are located in the apical positions. Jahn−Teller elongation of the bond distance is evident for these two apical atoms. Hydrogen bonds between the coordinated water molecule and the counterion are found in the crystal structures of complexes **3** and **5**.

Figure 4 demonstrates the absolute configuration of the anomeric oxygen atoms coordinated to the copper center and the chelate-ring conformations involving the anomeric oxygen atom. The results are summarized in Table 2. As reported earlier,[39] the metal coordination environments of complexes **1** and **2** are mirror images. Although complexes **3** and **5** both crystallize in a six-coordinate form with an *R* configuration for the oxygen center, complex **3** adopts a δ-gauche conformation for the five-membered chelate ring, whereas complex **5** crystallizes in a λ-gauche conformation. As a result, complex **5** has a configuration similar to that of complex **1** for the chiral environment around the copper center (Table 2).

Electronic Absorption Spectra. Table 3 shows the

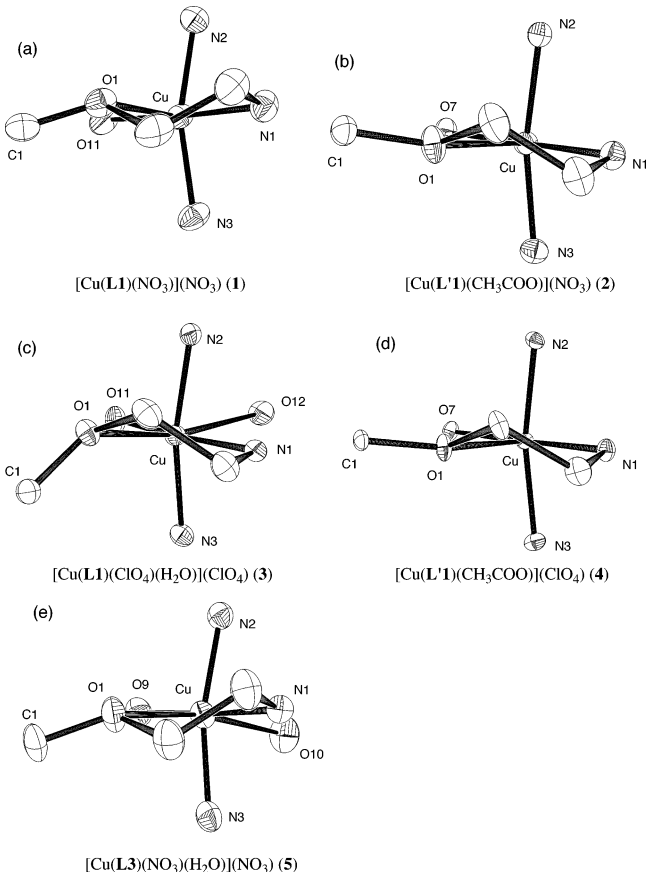

Figure 4. Coordination environment of the copper center in complexes **1**−**5** in the crystal structure: (a) [Cu(**L1**)(NO_3)](NO_3) (**1**), (b) [Cu(**L′1**)(CH_3COO)](NO_3) (**2**), (c) [Cu(**L1**)(ClO_4)(H_2O)](ClO_4) (**3**), (d) [Cu(**L′1**)(CH_3COO)](ClO_4) (**4**), (e) [Cu(**L3**)(NO_3)(H_2O)](NO_3) (**5**).

(66) Kirin, S. I.; Dübon, P.; Weyhermüller, T.; Bill, E.; Metzler-Nolte, N. *Inorg. Chem.* **2005**, *44*, 5405.
(67) Kirin, S. I.; Happel, C. M.; Hrubanova, S.; Weyhermüller, T.; Klein, C.; Metzler-Nolte, N. *Dalton Trans.* **2004**, 1201.
(68) Ishikawa, Y.; Ito, S.; Nishino, S.; Ohba, S.; Nishida, Y. *Z. Naturforsch. C: Biosci.* **1998**, *53*, 378.

Table 4. Structural Parameters Derived from EXAFS Analysis[a]

compound		N^b	r (Å)[c]	ΔE (eV)[d]	σ^e	R (%)[f]
complex **1**	Cu−N	4.1	1.992	0.795	0.058	2.455
		(4)	(1.984)			
powder	Cu−O	1.0	2.368	−4.401	0.060	
		(1)	(2.413)			
complex **3**	Cu−N	3.9	1.992	−0.053	0.056	1.310
		(4)	(1.984)			
powder	Cu−O	2.4	2.501	−4.573	0.081	
		(2)	(2.531)			
complex **1**	Cu−N	3.8	1.996	0.127	0.069	1.815
in MeOH	Cu−O	0.8	2.347	−2.120	0.083	
L2 + $Cu(NO_3)_2$	Cu−N	3.8	1.986	−0.875	0.060	1.092
in MeOH	Cu−O	0.7	2.359	−0.237	0.067	
L3 + $Cu(NO_3)_2$	Cu−N	2.8	1.984	−9.605	0.050	2.418
in MeOH	Cu−O	1.9	2.550	−5.143	0.080	

[a] Values in parentheses are derived from X-ray crystallography. [b] Coordination number. Estimated error is ±1. Coordination numbers are referenced to complexes 1 and **3** (powder). [c] Interatomic distance. [d] Shift of energy from E_0. [e] Debye−Waller factor. [f] $R = [\sum(k^3\chi_0(\mathbf{k}) - \mathbf{k}^3\chi_c(\mathbf{k}))^2/\sum(\mathbf{k}^3\chi_0(\mathbf{k}))^2]^{1/2}$. $\chi_0(\mathbf{k})$ and $\chi_c(\mathbf{k})$ are Fourier-filtered ($\Delta r = 0.8-2.9$ Å) and calculated data, respectively.

absorption data for mixed solutions of ligand and copper salt in methanol or water, including the data for complexes **1**−**5**. Job's plot reveals that **L1** coordinates to copper ion in 1:1 stoichiometry (Figure S1). For complexes **1** and **3**, the absorption spectra are in good agreement with those for the solution containing the corresponding ligand and metal salt. Consequently, the difference in absorption maxima of complexes **1** and **3** in methanol solution (648 vs 661 nm) is seen in corresponding ligand−metal mixed solution (651 vs 662 nm). Because the difference in these complexes (or ligand−metal mixed solutions) is the counterion, the counterion most likely exerts a small influence on the d−d transitions in methanol solution. On the other hand, in aqueous solution, no shifts in absorbance maximum were observed, and the absorption maximum at 660 nm suggests that the copper center can adopt a six-coordinate octahedral geometry coordinated to a water molecule similarly to complex **3**.

Complexes **2** and **4** exhibited slightly different absorption spectra than the associated ligand−metal mixtures. This can be explained by the fact that these complexes have an acetate ion coordinated to the copper center. The absorption spectrum of complex **5** also showed small differences from that of the ligand and metal mixture. Although these small exceptions exist, the present results indicate that the metal coordination environment of the equilibrium mixture of the ligand and metal in methanol solution is well described by the crystallized complex.

EXAFS Analysis. The X-ray absorption spectra around the Cu K edge were measured for powdered samples of complexes **1** and **3**, methanol solution of complex **1**, and ligand−$Cu(NO_3)_2$ mixtures for **L2** and **L3** in methanol. The Fourier transforms of the EXAFS oscillation are shown in Figures S2−5 (before phase correction), and the results are summarized in Table 4. All samples exhibited two different coordination modes of donor atoms in solid and solution. These were assigned to the backscattering contribution of nitrogen and oxygen atoms (N/O) coordinated to the copper center, corresponding to the in-plane donors with short (∼2.0 Å) bonds and the apical donor(s) with long (∼2.5 Å) bonds. The N/O atoms could not be distinguished in the present analysis. The longer bond (∼2.5 Å) is considered as a contribution from the intramolecular anomeric oxygen coordination to the copper center, which is evidenced from CD measurements (vide infra).

CD Spectra. Cotton effects were observed in the methanol and aqueous solutions of copper salts in the presence of **L1**−**3**, **L′1**−**3** (Figure 5), and complexes **1**−**5** (Figure 6) in the d−d transition region. These CD spectra indicate that the anomeric oxygen atom remains coordinated to the copper metal even in aqueous solution, leading to a chiral environment at the metal center. This coordination might be dynamic or in equilibrium; however, the ether oxygen-coordinated species make enough contribution to exhibit Cotton effects that otherwise cannot be observed. The EXAFS data also can be interpreted by the intramolecular ether oxygen coordination.

The CD behavior exhibited in Figures 5 and 6 can be categorized into the following three patterns (Figure 7): (a) a positive Cotton effect between 500 and 750 nm; (b) a negative Cotton effect between 500 and 750 nm; and (c) a positive Cotton effect between 500 and 600 nm, in combination with a negative Cotton effect in the 600−800-nm region. Pattern b is the mirror image of pattern a. The possible fourth pattern d, which is the mirror image of pattern c, will be discussed vide infra.

The most characteristic feature of the structure−Cotton effect relationship is that complexes **1** and **2**, which have an enantiomeric configuration in the solid state (i.e., Figure 4a,b or Table 2), exhibit a mirror-image Cotton effect (patterns a and b) in methanol solution. This observation indicates that the chiral environment around the copper center found in the crystal structures of the respective compounds is maintained in the methanol solution.

The octahedral complex **3** in methanol solution exhibited CD pattern c. This pattern is also present in an aqueous solution of the complex **1**, again suggesting that water coordination to the metal center occurs to generate a six-coordinate octahedral species. The same pattern is observed in a methanol solution of complex **1** containing 10% (v/v) water (data not shown).

Although complex **5** crystallizes as a six-coordinate structure, its CD spectrum in methanol solution resembles pattern a. This can be explained by the fact that the chiral environment around the metal center in **5** more closely resembles that in complex **1** than that in complex **3** in the crystal structure (Figure 4 and Table 2). The slight difference in CD spectra of **1** and **5** might originate from an equilibrium process involving the coordinated solvent or flexibility of the chelate ring in solution.

The other reported CD spectra might be a sum of an equilibrium mixture of several species in solution and are difficult to fully resolve; however, it should be noted that the Cotton effects observed are due to the coordination of the anomeric oxygen atom even in aqueous solution. Both α- and β-anomeric oxygens exhibited asymmetric coordination to the copper center. Sigel and co-workers demonstrated

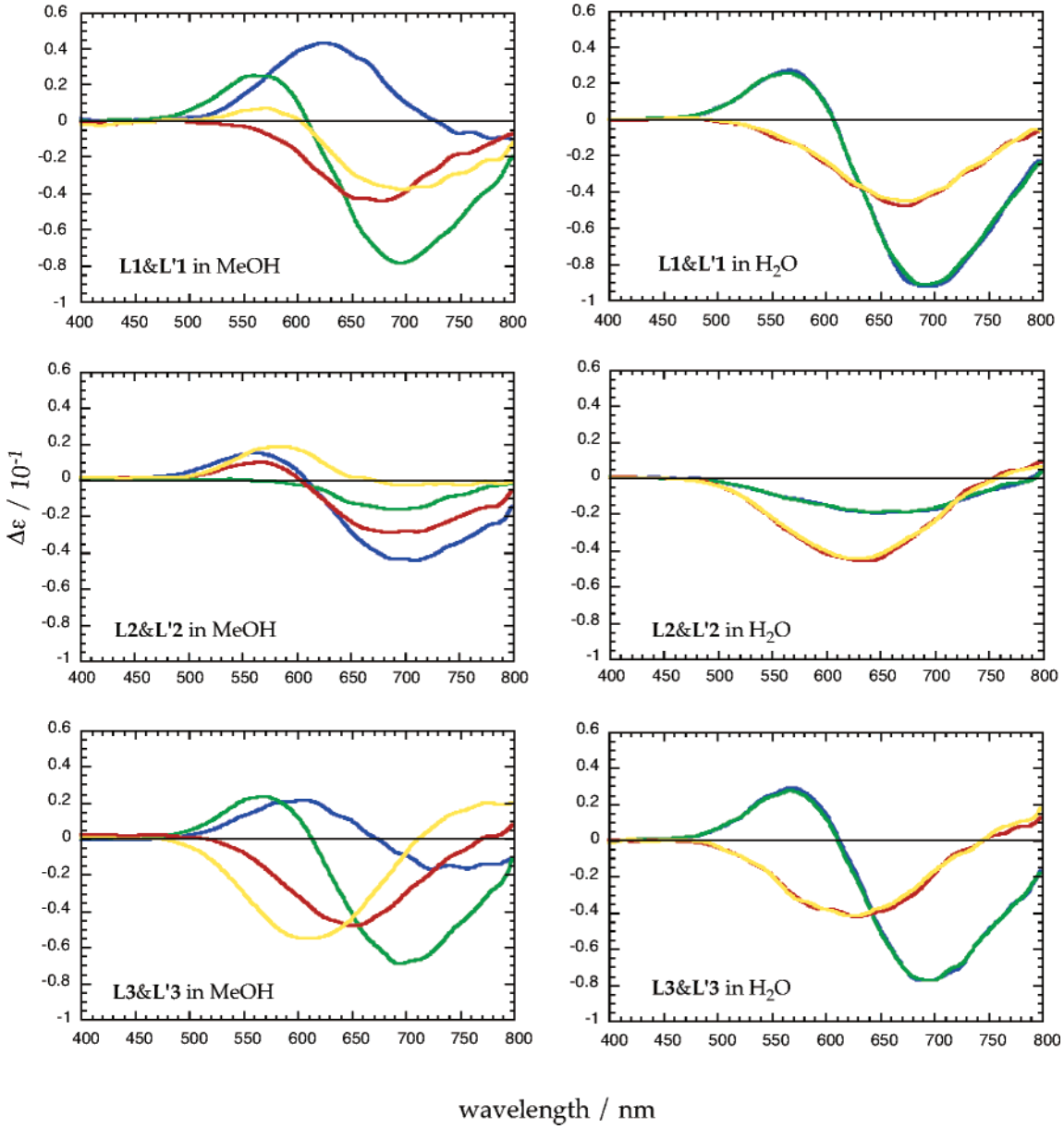

Figure 5. CD spectra of solutions containing 5.0 mM of ligands (**L1**−**3** and **L′1**−**3**) and copper salts in methanol (left panels) or water (right panels). Blue, **L** + $Cu(NO_3)_2$; green, **L** + $Cu(ClO_4)_2$; red, **L′** + $Cu(NO_3)_2$; yellow, **L′** + $Cu(ClO_4)_2$.

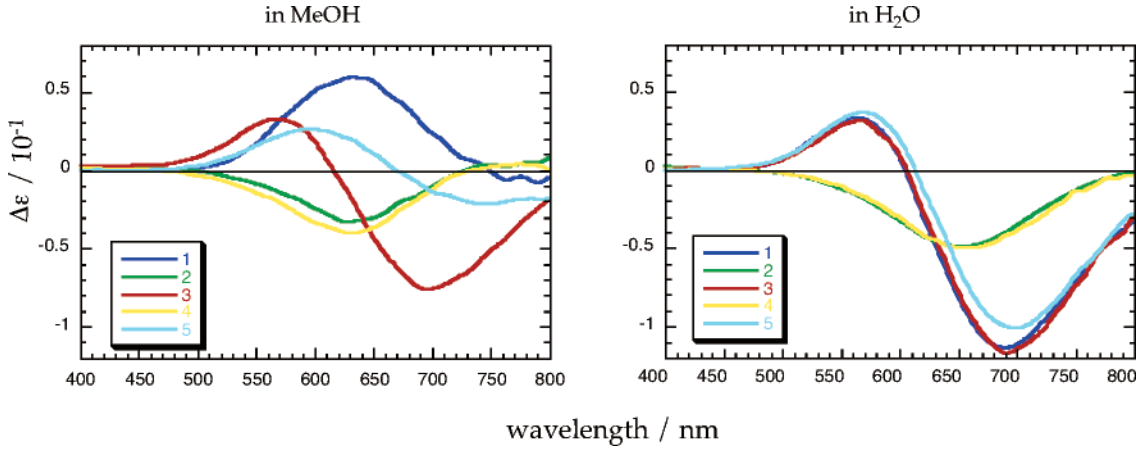

Figure 6. CD spectra of complexes **1**−**5** in methanol or aqueous solution.

the importance of the intramolecular equilibrium forming a five-membered chelate by the ether oxygen for metal complexes of phosphate ligands with an ether moiety in aqueous solution.[69−71] Similarly, in our system, the multi-

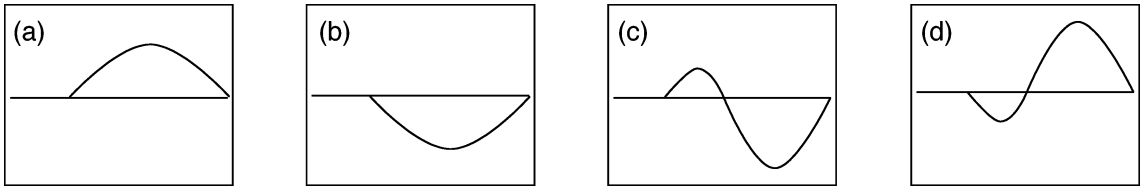

Figure 7. Schematic illustrations of CD spectra showing the typical patterns of the Cotton effects observed in Figures 5 and 6.

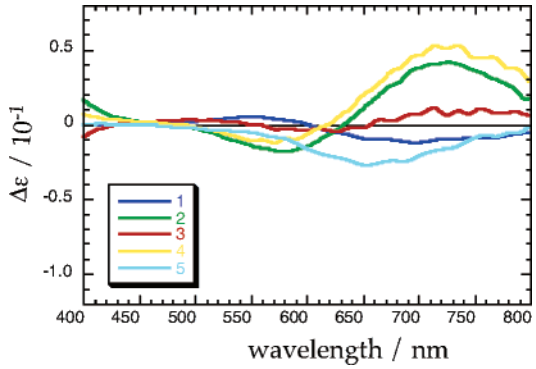

Figure 8. CD spectra of complexes **1**−**5** in pyridine solution.

dentate nature of **L** and **L′** most probably stabilizes the five-membered chelate ring involving the anomeric oxygen. This significant shift of the equilibrium toward intramolecular coordination of the anomeric oxygen, in cooperation with the chiral environment arising from the carbohydrate moiety, results in the active Cotton effect in solution.

Prompted by these results, we measured the CD spectra of complexes **1**−**5** in pyridine, a more coordinating solvent than water (Figure 8). Because of solubility characteristics, complexes **1** and **5** were measured in a water/pyridine mixed solution in 1:1 and 1:50 compositions, respectively. Interestingly, complexes **1** and **3** became CD-silent in pyridine solution; however, complexes **2**, **4**, and **5** were CD-active. Complexes **2** and **4** continued to exhibit significant Cotton effects, even in this highly coordinating solvent. These observations suggest that the DPA ligand exhibiting an acetylated glucose moiety tends to lose the anomeric oxygen coordination to the copper center in pyridine solution. In contrast, the deacetylated glucose derivative maintained the intramolecular ether oxygen coordination to the metal center. Moreover, pyridine solutions of complexes **2** and **4** show Cotton effect pattern d, indicating that the copper coordination environment exists as the mirror image of complex **3**, which shows pattern c in methanol and water. Although no crystals suitable for X-ray analysis of complexes **2** or **4** from pyridine solution have been isolated at this time, the free OH groups in the glucose moiety in these complexes are important for maintaining the intramolecular anomeric oxygen coordination and resulting chiral environment around the metal center.

(69) Sigel, H.; Kapinos, L. E. *Coord. Chem. Rev.* **2000**, *200*−*202*, 563.
(70) Sigel, H. *Chem. Soc. Rev.* **2004**, *33*, 191.
(71) Fernández-Botello, A.; Griesser, R.; Holý, A.; Moreno, V.; Sigel, H. *Inorg. Chem.* **2005**, *44*, 5104.

Conclusions

The copper(II) complexes **1**−**5** with a sugar-pendant DPA ligand were determined to exhibit asymmetric oxygen-atom coordination to the metal center in the solid state and in methanol, water, and pyridine solution. The absorption and CD spectra in solution are sensitive to the coordination environment around the copper center and were perturbed by changing the sugar moiety of the ligand, counterion, and solvent. Four distinct patterns were observed in the CD spectra, exhibiting two sets of mirror-image Cotton effects originating from the asymmetric configuration around the copper center. For complexes **1** and **2**, the configuration of the oxygen atom and the resultant chelate-ring conformation around the metal center were controlled by the protected/free hydroxyl groups of the sugar moiety. This is the first example of a pair of compounds that have structurally characterized asymmetric oxygen atoms with an enantiomeric configuration. The square-pyramidal/octahedral copper(II) centers also exhibited characteristic absorption and CD spectra. The interesting correlation between the Cotton effect in the CD spectra and the corresponding geometry of the copper center is still under investigation in our laboratory. The oxygen-atom chirality may be found in the catalytic mechanism of certain metalloenzymes, and could serve as a new concept for asymmetric catalyst design involving oxonium-assisted molecular transformations.

Acknowledgment. This work was supported by the Asahi-Glass Foundation; the Sasakawa Scientific Research Grant from the Japan Science Society; Nara Women's University Intramural Grant for Project Research; and Grant-in Aid for Scientific Research from the MEXT, Japan (16350032). The X-ray absorption spectral study was performed under the approval of the Photon Factory Program Advisory Committee (Proposal 2004G290). The authors thank Dr. Tim Storr of the University of British Columbia for critical reading of the manuscript and Professor Chikara Ohtsuki of Nara Institute of Science and Technology for elemental analyses.

Supporting Information Available: Job's plot, EXAFS data, and X-ray crystallographic data. This material is available free of charge via the Internet at http://pubs.acs.org.

IC051513F